Materials Science and Engineering A 396 (2005) 181–187

www.elsevier.com/locate/msea

HVOF spraying of nanostructured hydroxyapatite for biomedical applications

R.S. Lima [a,*], K.A. Khor [b], H. Li [b], P. Cheang [b], B.R. Marple [a]

[a] *National Research Council of Canada, 75 de Mortagne Blvd., Boucherville, Que., Canada J4B 6Y4*
[b] *School of Mechanical and Aerospace Engineering, Nanyang Technological University, 50 Nanyang Ave., Singapore 639798, Singapore*

Received 13 September 2004; received in revised form 6 January 2005; accepted 24 January 2005

Abstract

A nanostructured hydroxyapatite (HA) feedstock was thermally sprayed on Ti–6Al–4V substrates via high velocity oxy-fuel (HVOF process). The particle temperature and velocity for the HA particles in the HVOF jet were monitored during spraying and found to be $1826 \pm 346\,^{\circ}C$ and 638 ± 82 m/s, respectively. The bioactivity of the coating was investigated in a simulated physiological environment, as an attempt to simulate the real incubation condition of an implant in the human body, via immersing the coating in a simulated body fluid (SBF) for 7 days. The phase content and crystallinity of the coating was evaluated using X-ray diffraction (XRD). Field emission scanning electron microscopy indicated the presence of three types of nanostructured zones in the HA coating. The results show that the coating is highly crystalline and exhibits no secondary phases. After 7 days of incubation, a uniform layer of apatite ($\sim$35 μm) was formed over the HA coating surface, which was thicker than that found in early work on conventional air plasma sprayed HA coatings [R.S. Lima, B.R. Marple, K.A. Khor, H. Li, P. Cheang, Mechanical properties, microstructural characteristics and in vitro behavior of APS-sprayed nanostructured and conventional hydroxyapatite coatings, PDF file in the CD Proceedings of the International Thermal Spray Conference 2004, DVS-Verlag GmbH, Dusseldorf, Germany]. The HVOF-sprayed HA coating was dense and uniform, even surpassing the crystallinity levels and bond strength requirements of the standard ISO 13779-2 for HA coatings.

Keywords: Thermal spray; HVOF; Hydroxyapatite; Nanostructured coating; Bond strength

1. Introduction

The application of hydroxyapatite (HA) coatings on Ti-6Al–4V based prosthetics has been widely used due to the unique biocompatibility of HA. For a long term usage, an HA coating must exhibit a high biocompatibility and adequate mechanical properties, such as a high bond strength and an elastic modulus value close to that of the bone. The biocompatibility and the mechanical properties will depend on the coating microstructure, crystallinity and phase composition.

The air plasma spray (APS) technique has been used as the main process for applying HA coatings on titanium-based alloys. However, due to the extremely high temperatures of the plasma jet and the rapid cooling rate of sprayed particles [2], the degradation of HA during flight is inevitable [3–5]. The degradation of HA involves the formation of secondary phases, such as tricalcium phosphate (TCP), tetracalcium phosphate (TTCP), amorphous calcium phosphate (ACP) and calcium oxide - the latter not being biocompatible. The HA is a very stable phase in body fluids, but the secondary phases, particularly the ACP, have higher dissolution rates [6].

It has been generally accepted that high dissolution rates are unwanted because the dissolution of the secondary phases in the body fluids weakens the coating structure [4]. In order to achieve fixation with surrounding bone and a long life, the HA coating must have limited dissolution after implantation. Therefore the crystallinity of the coating is a very important parameter.

As mentioned above, ceramic materials, like HA, traditionally have been sprayed via air plasma spray (APS) due

* Corresponding author. Tel.: +1 450 641 5150; fax: +1 450 641 5105.
E-mail address: rogerio.lima@cnrc-nrc.gc.ca (R.S. Lima).

0921-5093/$ – see front matter.
doi:10.1016/j.msea.2005.01.037

to their high melting points and the high temperatures of the plasma jets [7]. However, it has been reported in the literature that when some ceramic coatings are deposited using high velocity oxy-fuel (HVOF) the respective coatings exhibit high microstructural uniformity, low porosity (<1%), high Weibull modulus values and superior wear behavior when compared to ceramics sprayed by APS [8–11]. Beyond these important enhancements it is important to point out that the jet of the HVOF systems has lower temperatures than those of the plasma jets [7]. This characteristic can be an important asset in order to suppress phase transformation during the spraying of HA [12].

Another important subject to be mentioned is nanomaterials. Recently the scientific community has focused considerable attention on these types of materials. It has been demonstrated that nanomaterials can exhibit enhanced hardness, strength, ductility, and toughness when compared to their conventional counterparts [13–15]. These characteristics open interesting possibilities in thermal spray. Indeed, it has already been shown that nanostructured thermal spray ceramic oxide coatings can have a superior wear performance when compared to similar coatings produced from conventional ceramic oxide powders [11,16–18].

To be successful in the air plasma spray processing of HA it is necessary to achieve a balance between two extremes. When HA is air plasma sprayed at low torch power (i.e., low particle temperature), the deposited coating exhibits low degradation, however, the mechanical properties are poor due to the lack of interlamellar contact (cohesion) within the coating microstructure. On the other hand, when HA is air plasma sprayed at high torch power (i.e., high particle temperature), its coating exhibits an improvement of the mechanical properties due to a better interlamellar contact, however, the formation of CaO reduces its biocompatibility [5].

With this in mind, the present study focused on employing the HVOF thermal spray process for producing HA coatings. This takes advantage of the low particle temperature and high particle velocity produced with this system, to deposit a coating with a high adhesion and cohesion. This results from the high kinetic energy of the particles at the point of impact with the substrate and the low level of degradation of the HA material due to the low particle temperature. The results of phase analysis, microstructure evaluation, in vitro behavior and bond strength measurement for this type of coating are analyzed.

2. Experimental procedure

2.1. Feedstock and spray process

The experimental nanostructured feedstock was prepared at Nanyang Technological University (Singapore) by reacting ortho-phosphoric acid with calcium hydroxide in a stoichiometric mole concentration and spray-drying of individual nano-sized particles of HA [19]. The particle size distribution of the feedstocks was determined via laser diffraction (Beckman Coulter LS 13320, Beckman Coulter, Miami, FL, USA). Thermal spraying of the feedstock was performed using an HVOF torch (DJ2700-hybrid, Sulzer-Metco, Westbury, NY, USA).

The temperature (T) and velocity (V) of the HA particles during thermal spraying were measured using a diagnostic tool based on pyrometric and time-of-flight measurements (DPV2000, Tecnar Automation, Saint Bruno, Que., Canada). The DPV2000 employs a two-color pyrometer (wave length: 700–1000 nm; temperature range: 200–4000 °C). The DPV2000 pyrometer was previously calibrated by using a tungsten lamp whose temperature had been previously measured by a pyrometer that was calibrated using a black body. The in-flight characteristics of a total of 1500 particles were evaluated. The T and V data were determined at the distance at which the substrate would normally be positioned when depositing a coating. Different sets of spray parameters were tested prior to depositing coatings. The parameter set that produced the highest average particle temperature was selected for coating production.

The coating was sprayed on Ti–6Al–4V substrates that had been grit-blasted with alumina to roughen the surface before spraying. The coating temperature was monitored using a pyrometer, which showed that the maximum coating temperature attained during deposition was ∼240 °C. The final thickness of the coatings was approximately 150 μm.

2.2. Characterization and analysis

The nanostructure and microstructure of the feedstock and coating were analyzed using a field-emission scanning electron microscope (S-4700, Hitachi, Tokyo, Japan). The coating porosity was measured via image analysis. A total of 10 cross-section pictures for each coating were analyzed. The phase composition and crystallinity were determined via X-ray diffraction (XRD; step: 0.01°, step time: 2.0 s). For determining crystallinity, a conventional feedstock (Captal 30, Plasma-Biotal Limited, Tideswell, North Derbyshire, UK) was used as the reference standard for calculation as it was sintered and did not show line-broadening effects. Both feedstocks exhibited 100% HA. The integrated intensities (area) of the peaks from 2θ 30 to 35° for the Captal 30 feedstock and the HVOF-sprayed coating were calculated. The respective crystallinity levels were then determined by dividing the integrated intensities of the coating by the integrated intensity of the Captal 30 feedstock [3].

The Kokubo simulated body fluid (SBF) [20] (pH = 7.40) was used for the in vitro incubation over 7 days. The solution is composed of 142.0 mM Na^+, 5.0 mM K^+, 1.5 mM Mg^{2+}, 2.5 mM Ca^{2+}, 147.8 mM Cl^-, 4.2 mM HCO_3^-, 1.0 mM HPO_4^{2-}, and 0.5 mM SO_4^{2-}. The in vitro test was conducted in a continuously stirred bath containing distilled

water with a stable temperature of 37 °C. Each sample was incubated in 70 ml SBF contained in a polyethylene bottle. Once the sample was removed from the solution, it was washed in distilled water and subsequently dried at ambient temperature.

2.3. Mechanical properties and residual stress

The Vickers microhardness of the coatings was measured by performing 10 indentations in the cross-section (centerline) using a 300 g load for 15 s. The bond strength was determined following a standard procedure (ASTM C633-01) for thermal spray coatings [21] using a universal testing machine.

To obtain some quantitative information on the residual stress condition of the coating, an Almen strip (type, N; grade, I) (Electronics Inc., Mishawaka, IN, USA) was mounted alongside the Ti–6Al–4V substrates and coated during the spraying process. The deflection of the Almen strip was read via an Almen gage (Model TSP-3, Electronics Inc., Mishawaka, IN, USA) before and after the coating deposition. The difference between these two values indicated whether the coating was in compression (negative value) or tension (positive value). This Almen procedure was based on a technique described by Sauer and Sahoo [22].

3. Results and discussion

3.1. Nanostructured feedstock and particle size distribution

Fig. 1 shows the nanostructured HA feedstock. It is observed that each feedstock particle of HA (Fig. 1a) is formed by an agglomeration of various individual nanosized particles of HA (Fig. 1b). The nanosized HA particles are elongated with lengths less than 500 nm and widths up to 100 nm. The particle size distribution of the feedstock can be found in Fig. 2. The majority of the particles have a diameter ranging from 5 to 50 μm.

3.2. In-flight particle characteristics and microstructure

The average particle velocity was 638 ± 82 m/s, whereas the average particle temperature was 1826 ± 346 °C. The distribution of particle temperature and velocity is shown in Fig. 3. It is observed that the particle temperature had a broader distribution than that of the particle velocity. The high velocities of the sprayed particles at the point of impact with the substrate or previously deposited layers resulted in a highly dense coating. The microstructure is shown in Fig. 4. It is possible to observe the low degree of porosity (porosity: 1.4 ± 0.1%) and the layered structure of the coating. The low jet temperatures of the HVOF flame (in comparison with a typical plasma jet temperature) led to the low degradation of the HA, as will be discussed in the next section.

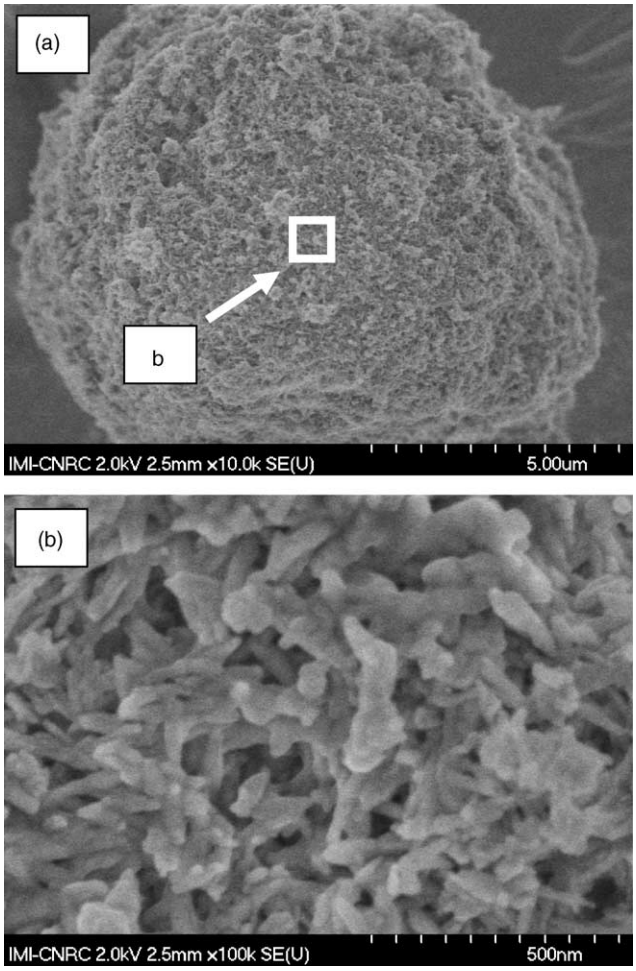

Fig. 1. HA microscopic particle (a) formed by the agglomeration of individual nanosized HA particles (b).

3.3. Phases and crystallinity

Fig. 5 shows the XRD patterns of the nanostructured HA feedstock and the HVOF-sprayed coating. Only HA peaks were detected, i.e., no secondary phases such as TCP, TTCP or CaO are present. The presence of two humps ($2\theta = 25°$–$35°$

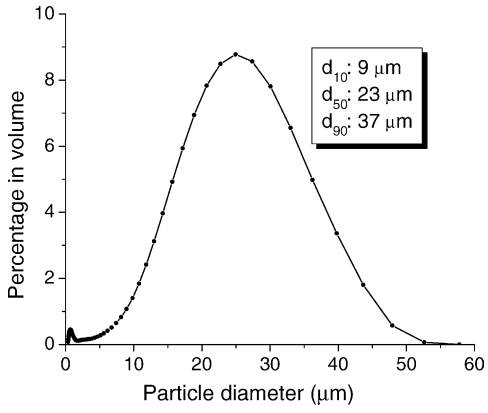

Fig. 2. Particle size distribution of the agglomerated HA feedstock particles.

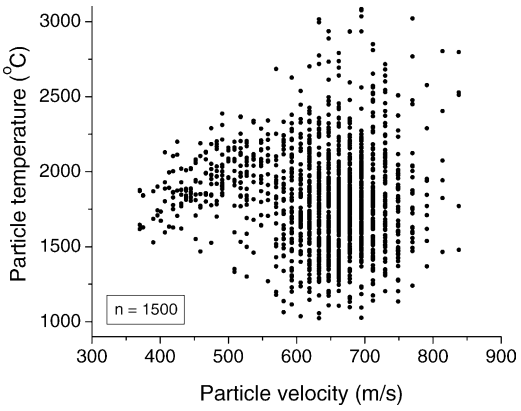

Fig. 3. Distribution of temperature and velocity of the HA particles in the HVOF jet.

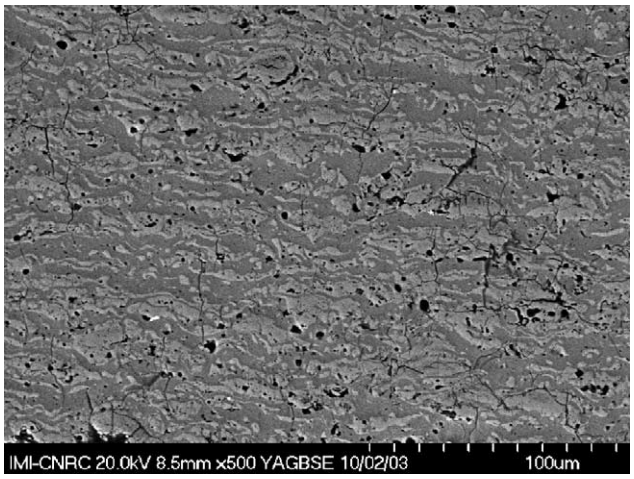

Fig. 4. Microstructure of the HVOF-sprayed HA coating.

and 45°–55°) indicates that some ACP is also present in the coating, however, the relative crystallinity of this coating was found to be 84%. It is important to remember that a high degree of crystallinity is a desirable characteristic for coating integrity because it implies a low percentage of the secondary phase ACP, which is unwanted due to its high dissolution rate in body fluids [5].

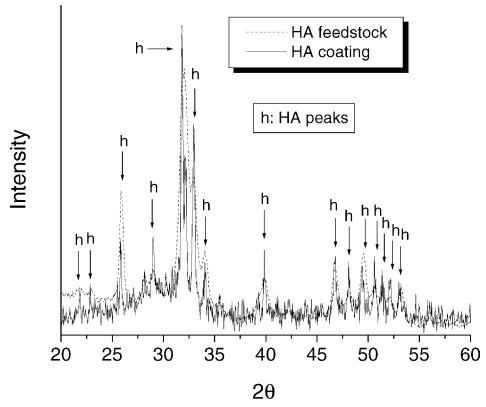

Fig. 5. XRD patterns of the nanostructured HA feedstock and its HVOF-sprayed coating.

According to Standard ISO 13779-2 [23], 'the crystalline content of HA shall be not less than 45% and the maximum allowable level of other crystalline phases shall be 5%, with the balance being amorphous.' Therefore the phase content and the crystallinity characteristics of the HVOF-sprayed HA coating made from the nanostructured feedstock surpass those demanded by the standard.

It is interesting to analyze this low degradation of the HA during HVOF spraying. According to the phase diagram for the system $CaO–P_2O_5–H_2O$, the HA decomposes at ∼1550 °C to a mixture of $Ca_3(PO_4)_2$ (TCP), $Ca_4P_2O_9$ (TTCP) and water [24]. The melting point of the mixture of TCP and TTCP formed by the decomposition of HA is ∼1570 °C. From the data available in Fig. 3, it is observed that many particles exhibit temperatures above 1550 °C. However, as was previously stated, the degradation of the HA coating was very low and its crystallinity was very high. These are strong indications that the majority of HA particles did not melt or undergo phase transformations during HVOF spraying. It is important to point out that these temperatures are measured via pyrometry, i.e., they represent surface values of temperature. Therefore the temperatures inside the particles may exhibit lower or higher values. Another point has to be added. Based on the particle velocity measurement and spray distance, the sprayed particles take less than a millisecond to travel from the torch to the substrate. As a consequence, the time exposure at high temperatures is very limited.

As previously mentioned, the nanostructured particles are very porous, with an enormous nanopore network (Fig. 1). It is not difficult to imagine that the thermal conductivity of the nanostructured particles is low due to the presence of a nanopore network. Therefore, the interior temperature of the nanostructured particles in the HVOF jet might be much lower than the temperature at the surface, thus producing less HA degradation.

Plastic deformation of HA particles at impact also needs to be considered as a possibility in order to explain how coatings were produced exhibiting both high mechanical integrity and low degradation of the HA. Hydroxyapatite has a hexagonal lattice with the space group $P6_3/m$ and isomorphous with fluorapatite. HA is believed to show analogous plastic behavior to fluorapatite on the basis of its crystal structure. Since the fluorapatite structure is stable up to the melting temperature, it has been employed for studying the mechanical property behavior at high temperatures [25]. In Ref. [25], the fluorapatite specimens were compressed using a universal testing machine in the temperature range from 1100 to 1500 °C. Detectable yielding (i.e., plastic deformation) appeared at 1100 °C and it was observed that the yield stress decreased with increasing temperature. Based on those results it may be possible that HA particles heated to temperatures between 1100 and 1550 °C (i.e., below the degradation temperature) and traveling at relatively high velocities underwent plastic

deformation and subsequent adhesion/cohesion to the substrate and previously deposited layers on impact. Therefore, it is possible that a significant part of the coating was formed without particle melting, thereby limiting the degradation of the HA coating.

3.4. Bond strength and residual stress

The bond strength of the HVOF-sprayed HA coating was 24 ± 8 MPa ($n = 5$). This average bond strength is higher than bond strengths of HA coatings deposited via air plasma spray, which generally exhibited bond strengths values below 20 MPa [3]. The bond strength of the HVOF-sprayed HA coating is also higher than the bond strengths of vacuum plasma sprayed HA coatings, which exhibited bond strengths from 4 to 14 MPa [26]. According to the standard ISO 13779-2 [23] 'the bond strength of an HA coating shall have a value not less than 15 MPa.' Therefore the HVOF-sprayed coating made from the nanostructured feedstock surpassed the standard.

The Almen strip exhibited a negative value of deflection after spraying. Therefore the HA coating is under a compressive stress. This characteristic is desirable because it inhibits crack propagation throughout the coating microstructure, however, very high levels of compressive stress may lower the bond strength of the coating.

3.5. Nanostructure of the coating

Different nanostructured zones were observed in the coating structure. Fig. 6 shows the cross-section of the HA coating. Two distinct nanostructured zones are found (Fig. 6b and c). The zone shown in Fig. 6b is porous, like the porous structure of the HA feedstock particle (Fig. 1b). It is thought that Fig. 6b represents an HA particle that was partially molten at impact with the substrate. The individual nanosized particles of the feedstock became rounded but they did not coalesce during spraying. Therefore the porous structure of the agglomerated feedstock was kept intact. Fig. 6c exhibits a nanostructured fibrous zone. It is possible to distinguish rounded particles embedded in the fibers, which indicate that probably this region was partially molten and there was some coalescence during flight or at impact.

Fig. 7 shows another type of nanostructure. It is possible to observe nanosized spherical particles densely packed, which were probably formed by the melting and coalescence of the elongated nanosized particles of the feedstock.

The presence of these different types of nanostructure should play an important role in increasing the bioactivity of the HA coating. It has been demonstrated that HA with a nanocrystalline structure exhibits enhanced bioactivity, i.e., the bone-bonding ability [27]. Even bioinert materials, such as alumina, start to exhibit bioactivity via the interaction with osteoblasts when certain nanostructural characteristics, such a nanoporosity, are present [28]. According to Webster et al. [29], osteoblast proliferation was significantly greater on nanophase alumina, titania and HA than on conventional formulations of the same ceramic.

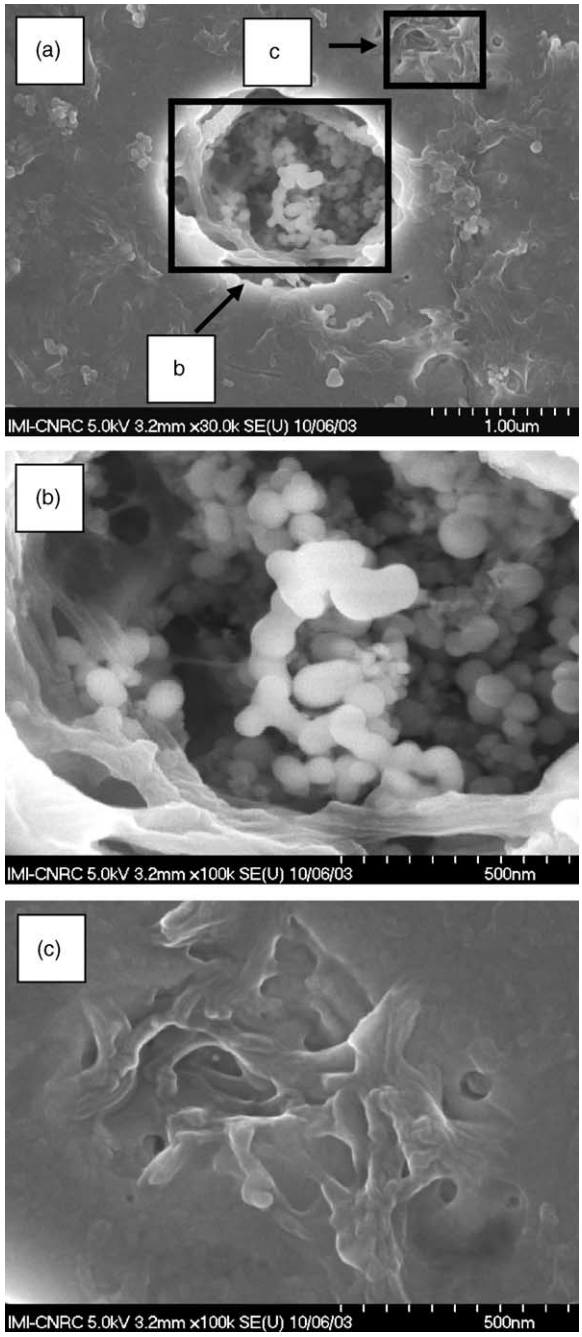

Fig. 6. Cross-section of the HA coating (a) showing a porous (b) and a fibrous (c) nanostructured zones.

3.6. In vitro behavior

Typically, the coating sample was incubated in the SBF for 7 days to reveal its dissolution/precipitation behavior. The topographical morphology of the coating after the in vitro incubation is shown in Fig. 8. After 7 days of incubation, the precipitation of the bone-like apatite layer is observed.

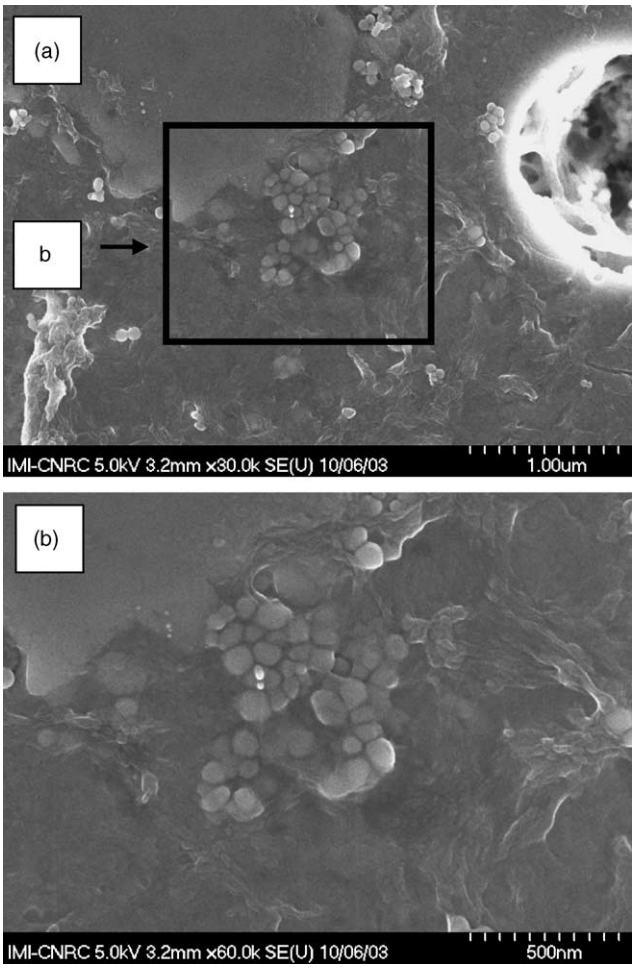

Fig. 7. Cross-section of the HA coating (a) showing a packed nanostructured zone (b).

Generally, the in vitro behavior of calcium phosphate coatings essentially involves a dissolution/precipitation process. The present coating has shown obvious precipitation after the 7 days immersion. Fig. 9 shows the cross-section of the

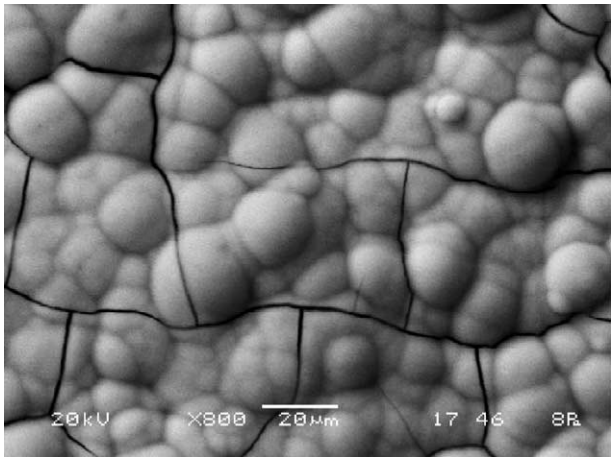

Fig. 8. Top surface of the HA coating after a 7-day incubation in the SBF solution.

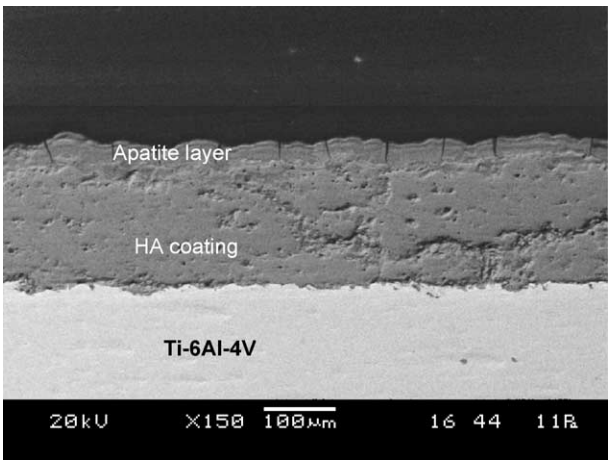

Fig. 9. Cross-section of the HA coating after a 7-day incubation in the SBF solution.

coating after the SBF incubation. It can be observed that an apatite layer with a thickness of approximately 35 μm formed over the HVOF-sprayed coating, which indicates a good bioactivity of the coating. It is possible to observe cracks of about 1 μm in width that formed in the apatite layer (see Figs. 8 and 9) as well as the formation of a dune-like surface morphology. The formation of these superficial dune-like surfaces and cracks has been reported previously [4,30]. The occurrence of these cracks is believed to be the result of diffusion and reaction between the coating surface and the SBF [30].

It is important to point out that, as reported in earlier work [1], a conventional air plasma sprayed HA coating was also incubated in the SBF for 7 days to reveal its dissolution/precipitation behavior. This resulted in the formation of an apatite layer with a thickness of approximately 20 μm over the air plasma sprayed conventional HA coating. Therefore, under the same SBF testing conditions, the HVOF-sprayed nanostructured HA coating seems to indicate, at least qualitatively, higher biocompatibility.

Several studies have pointed out the importance of an early dissolution/precipitation of HA coatings during apposition of bony tissues onto the implants [31,32]. The favorable effect on bone apposition on the HA implant gives evidence that this is due to early adhesion of osteoblasts and direct deposition of bone matrix on the HA substrate [32]. Thus, an early precipitation can be beneficial. However, unfortunately, a thorough understanding of the dissolution/precipitation behavior of the nanostructured HA is still lacking. The present results would suggest accelerated nucleation of the apatite on the nanostructured HA. Further work needs to be conducted to clarify the precipitation mechanism of the bone-like apatite on nanostructured HA.

4. Conclusions

- The HVOF-sprayed HA coating made from a nanostructured feedstock exhibited high crystallinity levels (84%)

and low degradation, without the presence of TCP, TTCP or CaO phases.

- The high crystallinity and low degradation of the HA coating were probably the result of (i) the low temperatures of the HVOF flame, (ii) the nanoporosity network of the HA feedstock particles (low thermal conductivity of the agglomerates) and (iii) a possible plastic deformation of the HA particles between 1100 and 1550 °C (i.e., below the degradation temperature and melting point).
- The HVOF-sprayed HA coating made from the nanostructured feedstock exhibited high density and microstructural uniformity.
- Three types of nanostructures with distinct morphologies were observed. The distinct morphologies were formed during spraying and impact via (i) melting without coalescence of the individual nanosized particles, forming a porous structure, (ii) melting and coalescence of individual particles, forming a packed structure and (iii) the formation of nanofibers from molten nanoparticles.
- A uniform layer of apatite (∼35 μm) was formed on the HA coating after 7 days of incubation in SBF. Comparing to previous results [1], an air plasma sprayed conventional HA coating, under the same SBF testing conditions, exhibited an apatite layer of ∼20 μm. This characteristic apparently indicates (qualitatively) a higher bioactivity and an accelerated nucleation of the apatite on the HVOF-sprayed nanostructured HA coating.
- The HVOF-sprayed HA coating exhibited high bond strength (24 ± 8 MPa). This bond strength value is higher than those generally found in the literature for air plasma sprayed and vacuum plasma sprayed conventional HA coatings.

References

[1] R.S. Lima, B.R. Marple, K.A. Khor, H. Li, P. Cheang, Mechanical properties, microstructural characteristics and in vitro behavior of APS-sprayed nanostructured and conventional hydroxyapatite coatings, in: Proceedings of the International Thermal Spray Conference, DVS-Verlag GmbH, Dusseldorf, Germany, 2004 (PDF file in the CD).

[2] L. Pawlowski, The Science and Engineering of Thermal Spray Coatings, Wiley, Chichester, England, 1995.

[3] S.W.K. Kweh, K.A. Khor, P. Cheang, Biomaterials 21 (2000) 1223–1234.

[4] S.W.K. Kweh, K.A. Khor, P. Cheang, Biomaterials 23 (2002) 775–785.

[5] L. Sun, C.C. Berndt, C. Grey, Mater. Sci. Eng. A 360 (2003) 70–84.

[6] L. Cleries, J.M. Fernandez-Pradas, G. Sardin, J.L. Morenza, Biomaterials 19 (1998) 1483–1487.

[7] P. Fauchais, Engineered Materials Handbook, in: S.J. Schneider Jr. (Ed.), Ceramic and Glasses, vol. 4, ASM International, Materials Park, OH, USA, 1991, pp. 202–208.

[8] R.S. Lima, B.R. Marple, J. Therm. Spray Technol. 12 (2) (2003) 240–249.

[9] R.S. Lima, B.R. Marple, J. Therm. Spray Technol. 12 (3) (2003) 360–369.

[10] Y. Liu, T.E. Fischer, A. Dent, Surf. Coat. Technol. 167 (1) (2003) 68–76.

[11] R.S. Lima, L. Leblanc, B.R. Marple, Abrasion behavior of nanostructured and conventional titania coatings thermally sprayed via APS, VPS and HVOF, in: Proceedings of the International Thermal Spray Conference, DVS-Verlag GmbH, Dusseldorf, Germany, 2004 (PDF file in the CD).

[12] K.A. Khor, H. Li, P. Cheang, Biomaterials 24 (2003) 2233–2243.

[13] C.C. Koch, D.G. Morris, K. Lu, A. Inoue, MRS Bull. (1999) 54–58.

[14] R. Vaβen, D. Stover, J. Mater. Process. Technol. 92–93 (1999) 77–84.

[15] Y. Lu, P.K. Liaw, J. Met. (2001) 31–35.

[16] M. Gell, E.H. Jordan, Y.H. Sohn, D. Goberman, L. Shaw, T.D. Xiao, Surf. Coat. Technol. 146–147 (2001) 48–54.

[17] L. Leblanc, in: B.R. Marple, C. Moreau (Eds.), Thermal Spray 2003: Advancing the Science and Applying the Technology, ASM International, Materials Park, OH, USA, 2003, pp. 291–299.

[18] G. E. Kim, J. Walker Jr., J. B. Williams Jr., US Patent 2003/0049449 A1 - Nanostructured titania coated titanium, March 13, 2003.

[19] S.W.K. Kweh, K.A. Khor, P. Cheang, J. Mater. Process. Technol. 89–90 (1999) 373–377.

[20] T. Kokubo, H. Kushitani, C. Ohtsuki, S. Sakka, T. Yamamuro, J. Mater. Sci.: Mater. Med. 3 (1992) 79–83.

[21] Standard test method for adhesion and cohesion strength of thermal spray coatings. ASTM C633-01, West Conshohocken, PA, USA.

[22] J.P. Sauer, P. Sahoo, in: C.C. Berndt, K.A. Khor, E.F. Lugscheider (Eds.), Thermal Spray 2001: New Surfaces for a New Millenium, ASM International, Materials Park, OH, USA, 2001, pp. 791–796.

[23] ISO 13779-2 Implants for surgery – hydroxyapatite – part 2: coating of hydroxyapatite. International Organization for Standardization.

[24] R. McPherson, N. Gane, T.J. Bastow, J. Mater. Sci.: Mater. Med. 6 (1995) 327–334.

[25] T. Nakano, T. Awazu, Y. Umakoshi, Scripta Materialia 44 (2001) 811–815.

[26] Y.C. Tsui, C. Doyle, T.W. Clyne, Biomaterials 19 (1998) 2015–2029.

[27] J. Ma, H. Wong, L.B. Kong, K.W. Peng, Nanotechnology 14 (2003) 619–623.

[28] M. Karlsson, E. Palsgard, P.R. Wilshaw, L. Di Silvio, Biomaterials (2003) 3039–3046.

[29] T.J. Webster, C. Ergun, R.H. Doremus, R.W. Siegel, R. Bizios, Biomaterials 21 (2000) 1803–1810.

[30] D.M. Liu, H.M. Chou, J.D. Wu, J. Mater. Sci.: Mater. Med. 5 (1994) 147–153.

[31] D.C.R. Hardy, P. Frayssinet, P.E. Delince, Eur. J. Orthop. Surg. Traumatol. 9 (1999) 75–81.

[32] U.E. Pazzaglia, F. Brossa, G. Zatti, R. Chiesa, L. Andrini, Arch. Orthop. Trauma. Surg. 117 (1998) 279–285.